



Contents lists available at ScienceDirect

Bioorganic & Medicinal Chemistry Letters

journal homepage: www.elsevier.com/locate/bmcl

Antitumor activity of deoxypodophyllotoxin isolated from *Anthriscus sylvestris*: Induction of G2/M cell cycle arrest and caspase-dependent apoptosis

Yeonjoong Yong^a, Soon Young Shin^b, Young Han Lee^{b,*}, Yoongho Lim^{a,*}^a Division of Bioscience and Biotechnology, BMIC, RCD, Konkuk University, Seoul 143-701, Republic of Korea^b Department of Biomedical Science and Technology, RCTC, Konkuk University, Seoul 143-701, Republic of Korea

ARTICLE INFO

Article history:

Received 3 March 2009

Revised 18 May 2009

Accepted 20 May 2009

Available online 28 May 2009

Keywords:

Anthriscus sylvestris

Apoptosis

Cell cycle arrest

Deoxypodophyllotoxin

ABSTRACT

An active compound having antitumor activity was isolated from the root of *Anthriscus sylvestris*. Structural studies revealed that it was deoxypodophyllotoxin (DPPT), and its biological activity was evaluated in HeLa human cervix carcinoma cells. Flow cytometric analysis showed that DPPT arrests the cell cycle in the G2/M phase prior to apoptosis. The mechanisms of action of DPPT involve inhibition of tubulin polymerization, dysregulation of cyclin A and cyclin B1 expression, and activation of caspases-3 and -7.

© 2009 Elsevier Ltd. All rights reserved.

Cancer is a leading cause of human death and can be triggered by environmental pollutants and genetic mutations. Traditional medicines have been shown to contain anticancer drugs such as camptothecin, taxol, and combretastatins.^{1–3} *Anthriscus sylvestris*, a medicinal plant, has been used in Korea for the prevention and treatment of various diseases, including bronchitis, and as an analgesic. One compound in *A. sylvestris* that has biological activity is a lignan, which has an estrogen-like chemical structure and functions as an inhibitor of topoisomerase II.^{4,5} Since topoisomerase II inhibition is one therapeutic strategy for cancer, many researchers have been interested in *A. sylvestris*. The major secondary metabolites in *A. sylvestris* are sylvestrin, 5-methoxypsoralen, scopoletin, falcariindiol,⁶ rutin,⁷ and epi-yangambin.⁴ Although the anti-insecticidal, antiviral, and antimitotic activities of *A. sylvestris* have been characterized, its effect on apoptosis has not been determined.^{8–10} Therefore, in this study, compounds from *A. sylvestris* that induce apoptosis were examined.

The dried root of *A. sylvestris* produced in Jeonnam Gurye, Korea, was purchased from a traditional medicine market in Seoul. Air-dried roots of the plant (1.2 kg) were ground into a fine powder and incubated with methanol (3 L, three times a day for 3 days) at room temperature in a dark room. After filtering, the methanol extracts were concentrated under reduced pressure with a rotor evaporator (Eyela, Tokyo, Japan). The concentrate was re-suspended with distilled water (1 L) and freeze-dried using liquid

nitrogen. The powdered methanol extract was re-suspended with distilled water (1 L) and then fractionated with hexane, chloroform, and ethyl acetate based on polarity. Each fraction was concentrated as described above for the methanol extract. Of the hexane, chloroform, ethyl acetate, and water fractions from the methanol extract, the chloroform fraction was subjected to further separation by column chromatography because it demonstrated the ability to induce apoptosis (Supplementary Fig. 1).¹¹ Apoptosis was analyzed by fluorescent activated cell sorting (FACS).¹² The chloroform fraction was separated via open column chromatography on a silica gel 60 stationary phase column (70–230 mesh; Merck, Whitehouse Station, NJ, USA); the compounds were purified by eluting with a mixed solvent consisting of hexane, chloroform, and ethyl acetate (3:1:2). Of the five fractions separated by column chromatography (Supplementary Fig. 2),¹¹ the second fraction (F2) showed strong apoptotic activity. This fraction was separated further using preparative high-performance liquid chromatography (HPLC; Varian, Palo Alto, CA, USA) on a reversed-phase C18 column (Gemini, 5 μ m, 10 \times 250 mm; Phenomenex, Torrance, CA, USA) with a UV/VIS detector (Varian), a mobile phase of 70% methanol in water, and a flow rate of 2.5 mL/min. The fraction collected at 11 min (F26) consisted of a single compound that had the highest apoptotic activity (Supplementary Fig. 3).¹¹ F26 (1 mg) was dissolved in a deuterated solvent (150 μ L) and transferred to a 2.5-mm NMR tube. All nuclear magnetic resonance (NMR) experiments were performed on an Avance 400 spectrometer system (9.4T; Bruker, Karlsruhe, Germany) at 298 K.¹³ Nineteen peaks were observed at the ¹³C NMR spectrum¹¹ (Supplementary Fig. 4), and their types were determined in distortionless enhancement by polarization

* Corresponding authors.

E-mail addresses: yhlee58@konkuk.ac.kr (Y.H. Lee), yoongho@konkuk.ac.kr (Y. Lim).

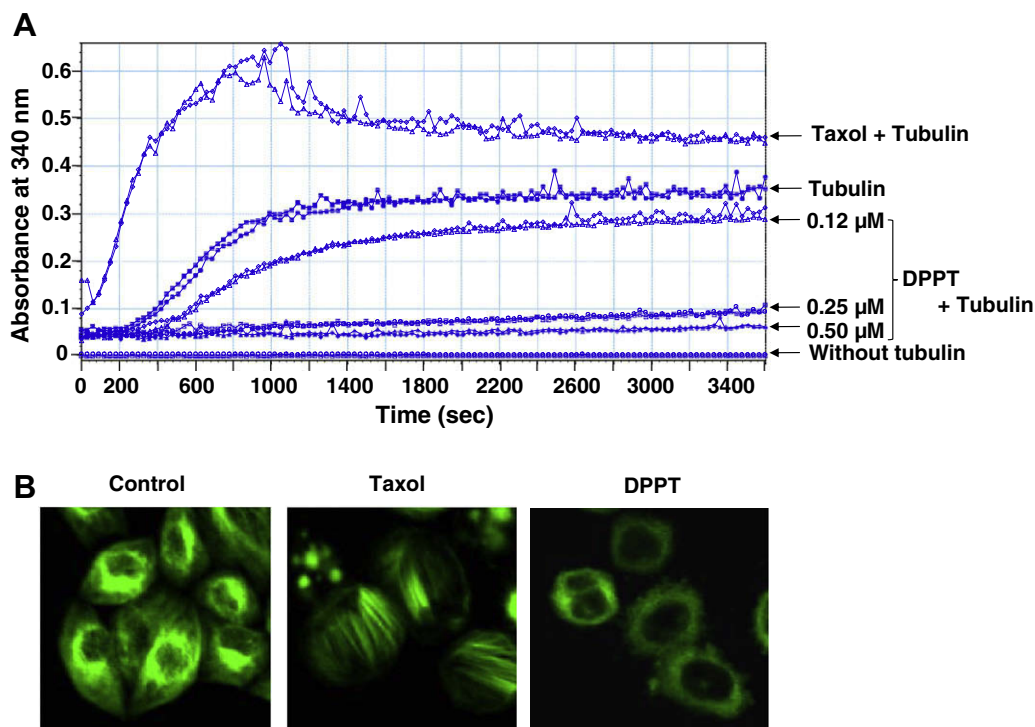


Figure 1. Effect of DPPT on microtubule assembly. (A) Tubulin in reaction buffer was incubated at 37 °C in the absence or presence of taxol (0.1 μ M) or the indicated concentration of DPPT. Absorbance was measured at 340 nm by spectrophotometry. (B) HeLa cells were treated with vehicle (DMSO), taxol (0.1 μ M), or DPPT (0.25 μ M) for 24 h. Microtubules were stained with an anti- α -tubulin antibody and an Alexa-Fluor 488-conjugated secondary antibody (Invitrogen, Carlsbad, CA, USA). The cellular microtubules were observed using an FV-1000 spectral confocal microscope (Olympus, Tokyo, Japan).

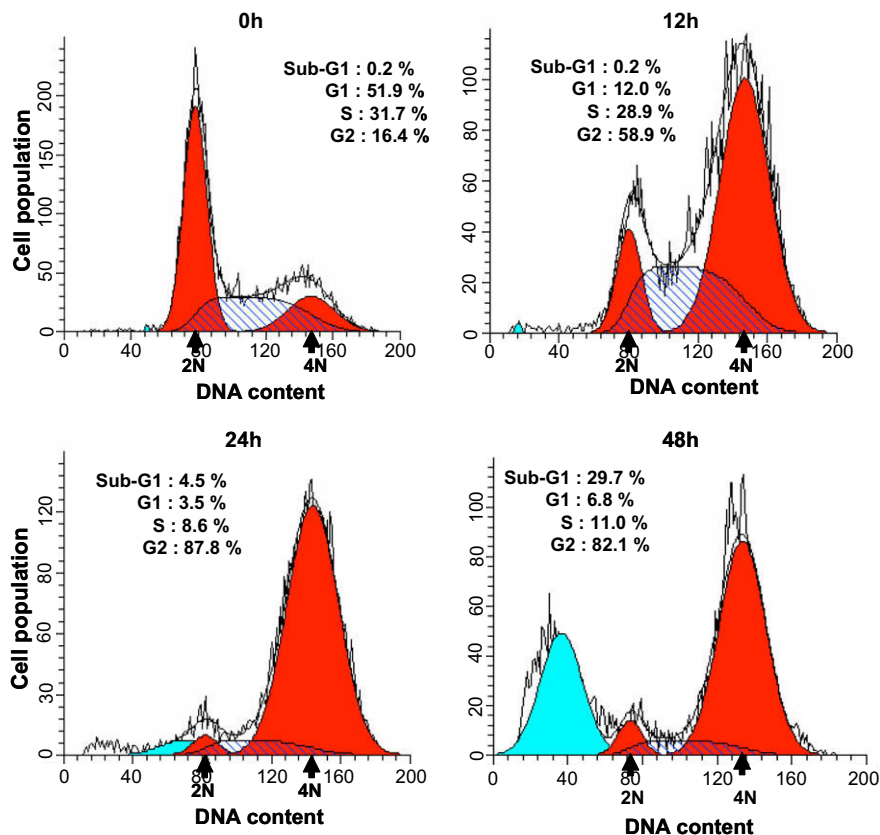


Figure 2. Effect of DPPT on cell cycle progression. HeLa cells were treated with DPPT (0.5 μ M) for the indicated times and analyzed for propidium iodide stained-DNA content by flow cytometry (FACS Calibur; Becton Dickinson Immunocytometry Systems, San Jose, CA, USA). Values indicate the percentage of the cell population at the phase of the cell cycle. The 2 N (diploid) and 4 N (tetraploid) DNA content represent the G1 and G2/M phases of the cell cycle, respectively. The population of cells in the sub-G1 phase represents cellular fragments due to apoptosis.

transfer (DEPT) experiments. Direct correlations between the ^1H and ^{13}C NMR data were determined by heteronuclear multiple quantum coherence (HMQC). Partial structures of the compound were obtained by interpreting correlation spectroscopy (COSY) and heteronuclear multiple-bond correlation (HMBC) data (Supplementary Fig. 5).¹¹ Based on the total assignments from the ^1H and ^{13}C NMR data (Supplementary Table 1),¹¹ the structure of the compound was determined to be deoxypodophyllotoxin (DPPT).¹⁴ To verify these results, mass spectrometry was performed.¹⁵ The spectrum indicated a strong sodium adduct peak at m/z 421 $[\text{M}+\text{Na}]^+$ (Supplementary Fig. 6).¹¹ A peak at m/z 819 was ascribed as being a dimer with a sodium adduct. The calculated molecular mass of 398 agreed with the NMR data and confirmed that the compound was DPPT.

All DPPT is a derivative of podophyllotoxin, a natural cyclolignan, and is known to inhibit tubulin polymerization.¹⁶ To determine whether DPPT isolated from the roots of *A. sylvestris* has a similar effect on tubulin, in vitro tubulin polymerization turbidity assays were performed.¹⁷ As shown in Figure 1A, when tubulin was polymerized in the presence of GTP at 37 °C, the absorbance at 340 nm increased with time. Addition of taxol, a reference compound that stabilizes microtubules, caused a marked increase in tubulin polymerization. In contrast, DPPT inhibited initiation of

tubulin polymerization in a concentration-dependent manner. These data demonstrate that isolated DPPT binds directly to tubulin, resulting in the inhibition of microtubule assembly. To extend these findings, we investigated whether isolated DPPT affects in vivo microtubular architecture (Fig. 1B). Microtubule assembly was analyzed by indirect immunofluorescence staining using an anti-tubulin antibody (Santa Cruz Biotechnology, Santa Cruz, CA, USA). Untreated HeLa cells (control) showed diffuse staining throughout the cytoplasm and dense perinuclear staining. Treatment with taxol resulted in a distinctive microtubule bundle that was likely due to stabilization of the rigid microtubule network. DPPT treatment, however, resulted in a loss of the microtubule network with short and peripheral bundles. These results suggest that DPPT isolated from the roots of *A. sylvestris* prevents microtubule assembly in vivo by inhibiting tubulin polymerization.

All inhibition of tubulin polymerization has been implicated in G2/M cell cycle arrest in various cancer cell lines.¹⁸ The effect of isolated DPPT on cell cycle progression was determined by FACS analysis in propidium iodide-stained HeLa cells. As shown in Figure 2, treatment with 0.5 μM DPPT led to a time-dependent accumulation of cells in the G2/M phase with a concomitant decrease in the population of G1 phase cells. G2/M phase arrest was initially detectable after 12 h of treatment; 58.9% of the cells

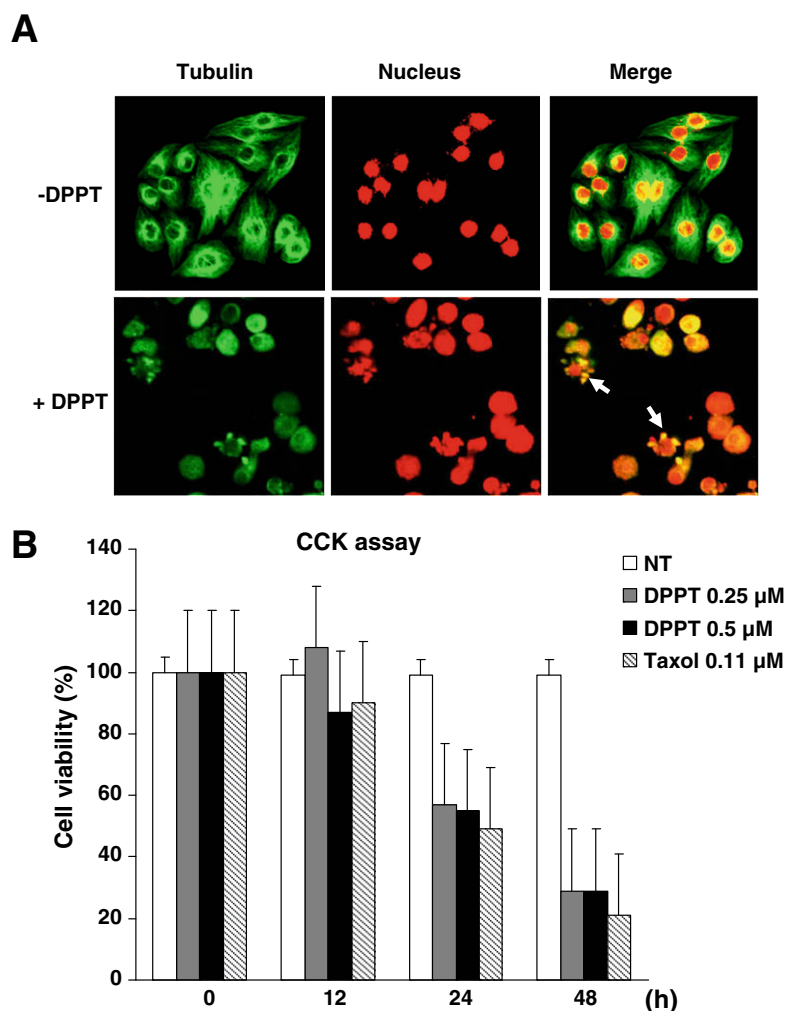


Figure 3. Effect of DPPT on the induction of cell death. (A) HeLa cells were treated with DPPT (0.5 μM) for 48 h. Microtubules (green) were stained with an anti- α -tubulin antibody and an Alexa-Fluor 488-conjugated secondary antibody. Chromosomal DNA (red) was stained with TO-PRO-3[®] iodide (Molecular Probes, Inc., Eugene, OR, USA). Arrows indicate the fragmented nuclei of apoptotic cells. (B) HeLa cells were seeded in 96-well culture plates and treated with various concentrations of DPPT for the indicated periods of time. The cellular survival rate was measured using Cell Counting Kit-8.¹⁹ Similar results were obtained from two other independent experiments.

were in G2/M phase compared to 16.4% in untreated cultures. Furthermore, the population of sub-G1 phase cells, a characteristic of apoptotic cells, was observed after 24 h of DPPT treatment; at time 0, only ~0.2% of the cells were in sub-G1 phase, while ~4.5% and ~29.7% of the cells were in sub-G1 phase after 24 h and 48 h, respectively. These data demonstrate that DPPT induces G2/M arrest before accumulation of cells in sub-G1 phase in HeLa cells.

To confirm the effect of DPPT on induction of apoptosis, fragmentation of chromosomal DNA was analyzed (Fig. 3A). Morphological changes were monitored by immunostaining with an anti-tubulin antibody. DNA staining demonstrated breakdown of nuclei and fragmentation of chromosomal DNA, both typical morphological features of apoptosis, after DPPT treatment. We next determined whether DPPT-induced apoptosis was associated with anti-proliferative activity. HeLa cells were treated with various concentrations of DPPT for 12, 24, and 48 h, and cell viability was analyzed using a Cell Counting Kit-8.¹⁹ As shown in Figure 3B, a significant decrease in cell survival was observed after 24 h with 0.25 μ M DPPT compared to untreated control cells. A similar effect was observed when cells were exposed to 0.1 μ M taxol.

Cell cycle progression is well established to be tightly regulated by the timing of the expression of cell cycle-specific cyclins. To determine the mechanism of DPPT-induced G2/M cell cycle arrest, we examined the effects of DPPT on the expression of cyclin A and cyclin B1, which control cell cycle progression through the S and G2/M phases, respectively. HeLa cells were treated with 0.5 μ M

DPPT for various time periods, and whole cell lysates were prepared for Western blot analysis.²⁰ GAPDH, a housekeeping gene, was used as an internal control. As shown in Figure 4A, treatment with DPPT resulted in a decrease in cyclin A expression. A rapid increase in cyclin B1 expression was observed within 3 h of DPPT treatment that remained elevated for up to 24 h; the expression of cyclin B1 returned to near control levels by 48 h. These data suggest that DPPT-induced cell cycle arrest at the G2/M phase is associated with its ability to alter the expression of cyclins A and B1. Caspases are cysteinyl aspartate proteinases that cleave substrate proteins at aspartate residues. Upon receiving an apoptotic signal, the precursor caspases undergo proteolytic processing to generate an active subunit. Among the 11 caspases characterized in humans, caspase-3 and -7 are the main downstream effector caspases that play essential roles in degrading the majority of key cellular components in apoptotic cells.²¹ We therefore investigated the possible involvement of caspases-3 or -7 in DPPT-induced apoptosis. The activation of caspases was monitored through detection of their proteolytic cleavage. Treatment of HeLa cells with 0.5 μ M DPPT promoted time-dependent cleavage of both caspase-3 and caspase-7 (Fig. 4B). The DNA repair enzyme poly(ADP-ribose)polymerase (PARP) is cleaved by caspase-3 or -7 from the full-length 116-kDa to an inactive 85-kDa form. To confirm the activation of caspase-3 or -7 by DPPT, we examined the generation of the apoptotic fragment of PARP. Western blot analysis revealed PARP cleavage 24 h after DPPT exposure; PARP cleavage due to DPPT was more extensive by 48 h. These data demonstrate the involvement of caspases-3 or -7 in DPPT-induced apoptosis.

Many ethnomedicines from plants contain biologically active compounds such as lignans, which are similar to estrogen in structure and inhibit topoisomerase II. Lignans in *A. sylvestris* have anti-insecticidal,²² antiviral, and antimutagenic activities that may be involved in the regulation of caspase-3,⁶ control of plant rooting,²³ antioxidant activity,²⁴ and inhibition of cardiovascular alterations and mortality due to endotoxins. Camptothecin, a widely used anticancer drug, contains an α -hydroxyl group on the lactone ring that is crucial for its anticancer effects.²⁵ The D-ring in DPPT, a five-membered lactone ring, may similarly contribute to its biological activity.

In summary, we isolated DPPT from the root of *A. sylvestris*. It displayed antitumor activity in HeLa cervix carcinoma cells. The mechanism of action of DPPT involve the inhibition of tubulin polymerization and dysregulation of cyclin A and cyclin B1 expression, thus resulting in the mitotic cell cycle arrest, and the activation of caspases-3 and -7, which promotes apoptotic cell death.

Acknowledgments

This work was supported by Grant KRF-2006-005-J03402 (KRF), Grant M10751050003-07N5105-00310 (KOSEF), Grant Biogreen 21 (RDA), and Agenda 11-30-68 (NIAS).

Supplementary data

Supplementary data associated with this article can be found, in the online version, at doi:10.1016/j.bmcl.2009.05.093.

References and notes

- Wall, M. E.; Wani, M. C.; Cook, C. E.; Palmer, K. H.; McPhail, A. I.; Sim, G. A. *J. Am. Chem. Soc.* **1966**, *88*, 3888.
- Wall, M. E.; Wani, M. C. *Cancer Res.* **1995**, *55*, 753.
- Pettit, G. R.; Sheo, B. S.; Boyd, M. R.; Hamel, E. *J. Med. Chem.* **1995**, *38*, 1666.
- Chao, Y. Y.; Jan, C. R.; Ko, Y. C.; Chen, J. J.; Jian, B. P.; Lu, Y. C.; Chen, U. C.; Su, W.; Chen, I. S. *Life Sci.* **2002**, *70*, 3109.
- Kashiwada, Y.; Bastow, K. F.; Lee, K. H. *Bioorg. Med. Chem. Lett.* **1995**, *5*, 905.

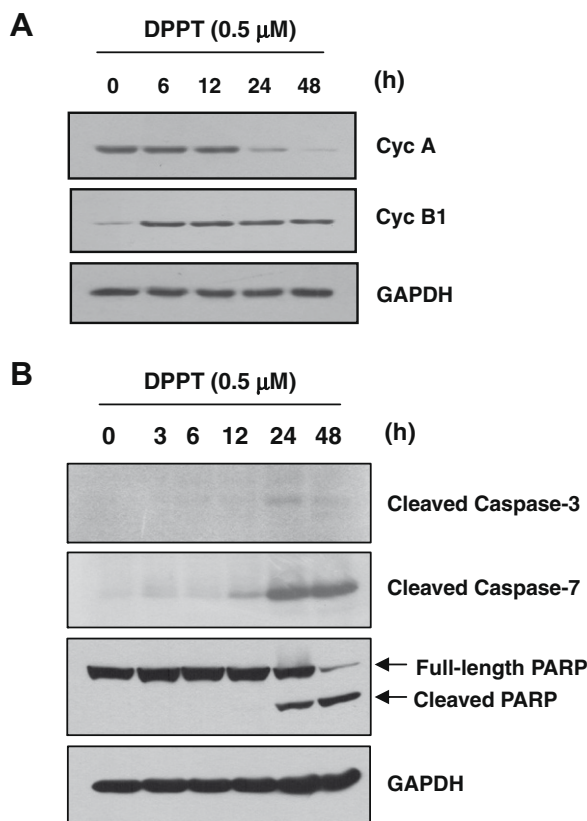


Figure 4. Effect of DPPT on the expression of cell cycle and apoptosis regulatory proteins. HeLa cells were treated with 0.5 μ M DPPT for the indicated times. Whole cell lysates were prepared and loaded for SDS-PAGE. After electrophoresis, proteins were transferred to blots and immunoreacted with the indicated antibodies. (A) Expression of S and G2/M regulatory proteins (cyclin A and cyclin B1). (B) Cleavage of apoptosis regulatory proteins (cleaved caspase-3, caspase-7, and PARP). Full-length PARP (116-kDa) and cleaved PARP (85-kDa) are indicated by arrows. GAPDH was used as an internal loading control.

6. Jeong, G. S.; Kwon, O. K.; Park, B. Y.; Oh, S. R.; Ahn, K. S.; Chang, M. J.; Oh, W. K.; Kim, J. C.; Min, B. S.; Kim, Y. C.; Lee, H. K. *Biol. Pharm. Bull.* **2007**, *30*, 1340.
7. Ng, T. B.; Liu, F.; Wang, Z. T. *Life Sci.* **2000**, *66*, 709.
8. Gao, R.; Gao, C.; Tian, L.; Ui, X.; Di, X.; Xiao, H.; Zahg, X. *Pest Manage. Sci.* **2004**, *60*, 1131.
9. Charltoh, J. L. J. *Nat. Prod.* **1998**, *61*, 1447.
10. Jordan, M. A.; Thrower, D.; Wilson, L. J. *Cell Sci.* **1992**, *102*, 401.
11. Data not shown in the text can be found in the [Supplementary Information](#).
12. For cell cycle arrest and apoptosis analysis, the HeLa cell line (CCL-2, cervical cancer cell) was cultivated at 37 °C in 5% CO₂ as suggested by the American Type Culture Collection (Manassas, VA, USA). The cells were grown in Dulbecco's modified Eagle's medium (DMEM) with fetal bovine serum (FBS) purchased from Gibco (Carlsbad, CA, USA). Cells (5×10^6) were seeded in 60-mm well plates and allowed to adhere for 24 h before treatment. The cells were treated with extracts and the pure compound was dissolved in 100% dimethyl sulfoxide (DMSO); DMSO was kept under 0.1% in the media in all control and treatment groups. After exposure to extracts or the pure compound, the cells were allowed to incubate for the indicated times. After 0, 12, 24, and 48 h, the control and treated cells were collected. The harvested cells were washed twice with phosphate-buffered saline (PBS), fixed in 70% ethanol, and stained with a 50 µg/ml propidium iodine (PI) solution and 100 µg/ml RNase-A at 37 °C in a dark room for at least 3 h. The cell cycle histogram data were produced by fluorescence activating cell sorting (BD Biosciences, San Jose, CA, USA). Apoptotic cells were counted as the percentage of cells in the sub-G1 phase, and data from cells arrested in the G2/M phase were used in cell cycle analysis.²⁶
13. General one-dimensional (1D) and two-dimensional (2D) NMR experiments were performed in methanol-*d*₄ and dimethyl sulfoxide-*d*₆. In the ¹H NMR analyses, 16 transients were acquired with 32 K data points. Its 90° pulse and spectral width were 9.5 µs and 4708 Hz, respectively. In the ¹³C NMR and distortionless enhancement by polarization transfer (DEPT) experiments, the 90° pulse and spectral widths were 10.5 µs and 22,075 Hz, respectively, and they were collected with 64 K data points. Correlated spectroscopy (COSY), heteronuclear multiple quantum coherence (HMQC), and heteronuclear multiple bonded connectivity (HMBC) experiments were acquired with 2048 data points for *t*₂ increments and 256 data points for *t*₁ increments. The long-range coupling delay for HMBC was 70 ms. Prior to Fourier transformation, zero-filling of 2 K and sine-squared bell window functions were applied using XWIN-NMR software (Bruker, Berlin, Germany).²⁷
14. Disuke, Y.; Hirohumi, O.; Mitsugi, K.; Yoshihiki, I.; Toshimasa, I.; Mastoshi, I. *Chem. Pharm. Bull.* **1988**, *36*, 3239.
15. Mass spectrometry was carried out using a 2D ion trap mass analyzer (Agilent, Chandler, AZ, USA) equipped with an autosampler, 1100 vacuum degasser, 1100 binary pump, a nanoflow LC system, orthogonal nanospray source, 1100 series LC/MSD trap module, a horizontally mounted triple flow turbo molecular pump, and a research grade mass detection system. Xcalibur 1.4 software was used for data processing. The mobile phase in LC was 50% methanol in water including 0.05% formic acid. The flow rate was 1 µL/min.
16. Loike, J. D.; Brewer, C. F.; Sternlicht, H.; Gensler, W. J.; Horwitz, S. B. *Cancer Res.* **1978**, *38*, 2688.
17. In vitro tubulin polymerization was assessed by the turbidity assay using the tubulin polymerization assay kit (Cytoskeleton, Denver, CO, USA; Cat. No. BK006 & CDS03) according to the manufacturer's instructions. Tubulin polymerization was monitored spectrophotometrically at 340 nm with gentle plate agitation. The absorbance values were measured at 30-s intervals for 60 min using a SpectraMAX 190 plate reader (Molecular Devices, Toronto, ON, Canada). Taxol was used as a positive control.²⁸
18. Vogel, S.; Kaufmann, D.; Pojarová, M.; Müller, C.; Pfaller, T.; Kühne, S.; Bednarski, P. J.; Angerer, E. *Bioorg. Med. Chem.* **2008**, *16*, 6436.
19. The time- and concentration-dependent effects of DPPT were assessed in triplicate. Following DPPT treatment, the cells were incubated under 5% CO₂ at 37 °C for an additional 24 h. After 24 h, water-soluble tetrazolium-8(2-(2-methoxy-4-nitrophenyl)-3-(4-nitrophenyl)-5-(2,4-disulphophenyl)-2H-tetrazolium, monosodium salt (Dojindo, Tokyo, Japan) was added to each well, and after 30 min, the optical density of each well was read at 450 nm.²⁶
20. Cyclin A, cyclin B1, PCNA, and glyceraldehyde 3-phosphate dehydrogenase (GAPDH) antibodies were purchased from Santa Cruz Biotechnology (Santa Cruz, CA, USA). Antibodies against PARP, cleaved caspase-3, and cleaved caspase-7 were obtained from Cell Signaling Technology (Beverly, MA, USA). HeLa cells were lysed in 20 mM HEPES (4-(2-hydroxyethyl)-1-piperazineethanesulfonic acid, pH 7.2), 1% Triton X-100, 10% glycerol, 150 mM NaCl, 10 µL/ml leupeptin, and 1 mM phenylmethanesulphonyl fluoride.¹³
21. Lakhani, S. A.; Masud, A.; Kuida, K.; Porter, G. A., Jr.; Booth, C. J.; Mehal, W. Z.; Inayat, I.; Flavell, R. A. *Science* **2006**, *311*, 847.
22. Araujo, C. V.; Barbosa Filho, J. M.; Cordeiro, R. S.; Tibirica, E. *Naunyn. Schmiedeberg's Arch. Pharmacol.* **2001**, *363*, 267.
23. Sirois, J. C.; Miller, R. W. *Plant Physiol.* **1972**, *49*, 1012.
24. Simic, A.; Manoilovic, D.; Segan, D.; Todorovic, M. *Molecules* **2007**, *12*, 2327.
25. Vandana, S.; Arvind, S. N.; Kumar, J. K.; Gupta, M. M.; Suman, P. S. *Bioorg. Med. Chem.* **2005**, *13*, 5892.
26. Choi, B. H.; Kim, C. G.; Bae, Y. S.; Lim, Y.; Lee, Y. H.; Shin, S. Y. *Cancer Res.* **2008**, *68*, 1369.
27. Kim, H.; Lee, E.; Kim, J.; Jung, B.; Chong, Y.; Ahn, J.-H.; Lim, Y. *Bioorg. Med. Chem. Lett.* **2007**, *18*, 661.
28. Gupta, M.; Bode, C.; Georg, G.; Himes, H. *Proc. Natl. Acad. Sci.* **2003**, *100*, 6394.